Microglia, Amyloid, and Glucose Metabolism in Parkinson's Disease with and without Dementia

Paul Edison*[1,7], Imtiaz Ahmed[1,7], Zhen Fan[1], Rainer Hinz[1,2], Giorgio Gelosa[1,3], K Ray Chaudhuri[4], Zuzana Walker[5], Federico E Turkheimer[1,4] and David J Brooks[1,6]

[1]Centre of Neuroscience, Department of Medicine, Imperial College London, London, UK; [2]Wolfson Molecular Imaging Centre, University of Manchester, Manchester, UK; [3]Department of Neurology, University of Milan-Bicocca, Milan, Italy; [4]MRC Centre of Neurodegeneration Research, Kings College London, London, UK; [5]Department of Mental Health Sciences, University College London, London, UK; [6]Hammersmith Imanet, GE Healthcare, London, UK

[11C](R)PK11195-PET measures upregulation of translocator protein, which is associated with microglial activation, [11C]PIB-PET is a marker of amyloid, while [18F]FDG-PET measures cerebral glucose metabolism (rCMRGlc). We hypothesize that microglial activation is an early event in the Parkinson's disease (PD) spectrum and is independent of the amyloid pathology. The aim of this study is to evaluate *in vivo* the relationship between microglial activation, amyloid deposition, and glucose metabolism in Parkinson's disease dementia (PDD) and PD subjects without dementia. Here, we evaluated 11 PDD subjects, 8 PD subjects without dementia, and 24 control subjects. Subjects underwent T1 and T2 MRI, [11C](R)PK11195, [18F]FDG, and [11C]PIB PET scans. Parametric maps of [11C](R)PK11195 binding potential, rCMRGlc, and [11C]PIB uptake were interrogated using region of interest and SPM (statistical parametric mapping) analysis. The PDD patients showed a significant increase of microglial activation in anterior and posterior cingulate, striatum, frontal, temporal, parietal, and occipital cortical regions compared with the controls. The PD subjects also showed a statistically significant increase in microglial activation in temporal, parietal, and occipital regions. [11C]PIB uptake was marginally increased in PDD and PD. There was a significant reduction in glucose metabolism in PDD and PD. We have also demonstrated pixel-by-pixel correlation between mini-mental state examination (MMSE) score and microglial activation, and MMSE score and rCMRGlc. In conclusion, we have demonstrated that cortical microglial activation and reduced glucose metabolism can be detected early on in this disease spectrum. Significant microglial activation may be a factor in driving the disease process in PDD. Given this, agents that affect microglial activation could have an influence on disease progression.

Neuropsychopharmacology (2013) **38**, 938–949; doi:10.1038/npp.2012.255; published online 16 January 2013

Keywords: amyloid; microglia; Parkinson's disease; Parkinson's disease dementia; glucose metabolism

INTRODUCTION

Around 80% of Parkinson's disease (PD) subjects develop dementia if they survive for 20 years with the condition and on average the prevalence is 40% (Cummings, 1988; Hughes *et al*, 2000). Parkinson's disease dementia (PDD) is characterized by impairment of short-term recall, attention, visuospatial, and executive functions. such as decision making (Emre *et al*, 2007). Cortical Lewy bodies, Alzheimer pathology, degeneration of subcortical nuclei, including the medial substantia nigra, the cholinergic nucleus basalis of Meynert, the noradrenergic locus ceruleus, and other brain stem nuclei or combination of these factors contribute to dementia in PDD.

Microglia constitute 10–15% of non-neuronal cells in the brain and normally are in a resting stage monitoring the brain milieu. Invading pathogens, trauma, infection, degenerative disease, and stroke can all trigger activation of microglia with the production and release of reactive oxygen and nitrogen species, cytokines, and chemokines. This intrinsic 'inflammation' in the central nervous system may have both beneficial as well as harmful effects (McGeer and McGeer, 2004; Wyss-Coray and Mucke, 2002). Chronic low levels of neuroinflamation may lead to progressive damage of the host tissue, and it is proposed that neuroinflamation is associated with all neurodegenerative disorders, including Alzheimer's disease (AD) and PD.

It has been suggested that the chronic inflammation mediated by microglial cells may contribute to the death of dopamine-producing neurons in the brain (Hirsch *et al*, 2003). In post-mortem studies, it is demonstrated that AD

*Correspondence: Dr P Edison, Clinical Senior Lecturer, Imperial College London, MRC Cyclotron Building, Hammersmith Hospital, Du Cane Road, London W12 0NN, UK
E-mail: paul.edison@imperial.ac.uk
[7]These authors contributed equally to this work.

β-amyloid fibrils are associated with activated microglia. As up to 40% of PDD subjects have significant amount of amyloid, it may be possible that cell loss could arise from the presence of dual pathology resulting in reduced cortical glucose metabolism (Berding et al, 2001; Eberling et al, 1994; Feng et al, 2008; Hosokai et al, 2009; Peppard et al, 1992; Sasaki et al, 1992; Yong et al, 2007). To date, no effective treatment is available to prevent the progression of PDD. For an effective treatment strategy, it is important to understand the relative roles of microglial activation and amyloid deposition, and influence of these on cerebral glucose metabolism.

Marked upregulation of mitochondrial translocator protein (TSPO) expression—also known as peripheral benzodiazepine-binding sites—is associated with microglial activation. [^{11}C](R)PK11195 (1-(2-chlorophenyl)-N-methyl-N-(1-methylpropyl)-3-isoquinoline carboxamide) positron emission tomography (PET) is a measure of upregulation of TSPO (Shah et al, 1994). In normal brain tissue, specific binding of [^{11}C](R)PK11195 is low as microglia are in a resting state. Autoradiography combined with immunocytochemical studies has shown that brain binding of [^{11}C](R)PK11195 closely follows the distribution of microglia activated by brain injury in conditions such as multiple sclerosis (Banati et al, 2000). Previous PET studies from our group have reported that increased [^{11}C](R)PK11195 binding could be detected in both idiopathic PD and AD subjects (Edison et al, 2008a; Gerhard et al, 2006).

[^{11}C]PIB (N-methyl-[11-C]2-(4'-methyl amino phenyl)-6-hydroxy benzothiazole), binds to fibrillar β-amyloid in both neuritic and non-neuritic plaques in the cortex and striatum of AD patients but not to amorphous β-amyloid deposits; the latter can be found in the cerebellum (Klunk et al, 2003). Studies have reported twofold increases in cortical uptake of [^{11}C]PIB inAD compared with healthy controls, and a significant proportion of healthy subjects have high amyloid (Edison et al, 2007; Klunk, 2011; Nordberg et al, 2010; Pike et al, 2007). Several studies are underway evaluating the progression of AD under Alzheimer's disease neuroimaging consortium (Weiner et al, 2012) and Australian Imaging Biomarkers and Lifestyle Flagship study of Ageing (Rowe et al, 2010).

To date, there has been no attempt to evaluate the relationship between microglial activation, amyloid deposition, and glucose metabolism in PD and PDD in vivo. Here we hypothesize that microglial activation has a significant role in this disease, is independent of the amyloid pathology, and is associated with reduction in glucose metabolism. In order to establish whether these neuropathological substrates are associated, we have used PET to quantify in vivo specific binding of [^{11}C](R)PK11195, [^{11}C]PIB, and [^{18}F]FDG in PDD subjects and in PD subjects without dementia and compared the results with those obtained for a group of normal subjects.

MATERIALS AND METHODS

Eleven PDD subjects, 8 PD subjects without dementia, and 24 control subjects were recruited from Imperial College NHS trust and the nearby London hospitals. Each PDD and PD subjects had three PET scans with [^{11}C](R)PK11195, [^{11}C]PIB, and [^{18}F]FDG. Ten age-matched healthy control subjects had [^{11}C](R)PK11195 PET scans, while eight had [^{18}F]FDG PET, and 14 healthy control subjects had [^{11}C]PIB PET scans. Six of the PDD subjects and PD subjects without dementia were recruited as part of a previously published study by our group (Edison et al, 2008b). All subjects had detailed neurological assessments, including a history from a close relative, routine blood analysis, and detailed neuropsychometric tests assessing verbal and visual memory, attention, executive, visuoconstruction, language, and recognition memory. Subjects were assigned a diagnosis of PDD based on consensus clinical diagnostic criteria (Emre et al, 2007). The inclusion and exclusion criteria for PDD, PD, and control subjects are same as previously described (Edison et al, 2008b). Dementia was excluded in control subjects and PD subjects without dementia by detailed clinical examination and psychometric testing while significant cerebral atrophy was excluded by T1-weighted MRI scan and structural damage by T2-weighted MRI scan. Permission to perform this study was obtained from the Ethics Committee of the Hammersmith Hospitals Trust while permission to administer radiotracers was obtained from the Administration of Radioactive Substances Advisory Committee (ARSAC), UK.

MRI Scanning

MRIs were obtained using a 1.5 Tesla GE scanner. T1 volumetric MRI (3D T1 volume, pulse sequence RF-Fast, acquisition times TR 30 ms, TE 3 ms, flip angle 30°, field of view 25 cm, matrix 156 × 256, voxel dimensions 0.98 × 0.98 × 1.6 mm.) were acquired for co-registration and assessment of atrophy while T2-weighted images were acquired to rule out any structural abnormality in PDD, PD, and control subjects.

PET Scanning

PET with [^{11}C](R)PK11195. Subjects underwent [^{11}C](R) PK11195-PET using high-resolution, high-sensitivity ECAT EXACT HR + + (CTI/Siemens 966) camera (Spinks et al, 2000) at Imperial College London. A 10-min transmission scan was performed for attenuation correction. Thirty seconds after the start of the emission scan, a mean dose of 296 (SD ± 18) MBq [^{11}C](R)PK11195 in 5 ml normal saline was injected intravenously over 10 s. Emission data were then acquired over 60 min in list-mode and rebinned into 18 time frames post acquisition.

PET with [^{11}C]PIB. All subjects had an intravenous bolus injection of [^{11}C]PIB (mean injected dose 370 (SD ± 20) MBq) and were scanned using a Siemens ECAT EXACT HR + scanner (Brix et al, 1997) as previously described (Edison et al, 2007). Dynamic emission scans were acquired in three-dimensional mode over 90 min. All data processing and image reconstruction were performed using standard Siemens software, which included scatter correction.

PET with [^{18}F]FDG. All PD and PDD subjects and healthy controls were scanned using a Siemens ECAT EXACT HR + scanner. Subjects were asked to fast for 4 h

before the bolus injection of 185 ($\pm$8) MBq of [^{18}F]FDG. A 60-min dynamic emission scan was acquired using a predefined protocol with time frames $1 \times 15\,s$, $1 \times 5\,s$, $4 \times 10\,s$, $4 \times 30\,s$, $4 \times 60\,s$, $4 \times 120\,s$, and $9 \times 300\,s$. All subjects had radial artery cannulation. Continuous online sampling was performed for 15 min and then discrete blood samples were taken at baseline, 5, 10, 15, 20, 30, 40, 50, and 60 min. A hematocrit was estimated from the baseline blood sample, and plasma glucose levels were measured on selected samples. Due to the blockage of arterial cannula, we were unable to estimate rCMRGlc in two PD subjects.

Analysis of PET Scan Data

Analysis of [^{11}C](R)PK11195-PET Data

Cluster analysis. Parametric images of [^{11}C](R) PK11195 binding potential (BP), reflecting B_{max}/K_d, were generated with a simplified tissue reference two brain compartmental model (SRTM). As PDD and PD patients have widespread distribution of pathological changes, no single region free of disease can be identified as a reference for non-specific tracer binding. Cluster analysis was, therefore, used to extract and identify a distributed cluster of voxels that mirrored a normal population cortical reference input function for each individual PDD and PD subject. We have introduced a novel computational methodology that enables the extraction of a reference cluster from [^{11}C](R)PK11195 dynamic PET studies (Turkheimer *et al*, 2007). The use of an appropriate reference not only increases the sensitivity of the quantification procedure to the specific signal from microglia but also minimizes the sensitivity of the calculated BP, obtained by the modeling procedure, to changes in blood flow. Our unit has validated use of the SRTM with a reference input function defined by cluster analysis as the most reproducible and sensitive technique for generating BP maps (Anderson *et al*, 2007).

Analysis of [^{11}C]PIB PET Data

Target region-to-cerebellum ratios (RATIO). Target region to cerebellar [^{11}C]PIB uptake ratio images were created by dividing integrated 60–90 min voxel tracer uptake by that of cerebellar gray matter as previously described (Edison *et al*, 2007). Target-to-cerebellar ratio at a later time point provides a blood flow independent measure of specific [^{11}C]PIB retention that is easy to calculate and does not require arterial sampling (Lopresti *et al*, 2005).

Analysis of [^{18}F]FDG-PET data. Parametric maps of absolute rCMRGlc were generated with spectral analysis using an arterial input function as previously described (Cunningham and Jones, 1993; Hu *et al*, 2000). We used a lumped constant of 0.48. For region of interest (ROI) analysis of [^{18}F]FDG scans, all the individual images were coregistered to their corresponding MRIs and then normalized to MNI space as described below.

ROI analysis. Parametric maps of [^{11}C](R)PK11195 BP maps were coregistered to the individuals' MRIs and spatially transformed into MNI space using SPM8, while [^{11}C]PIB uptake RATIO image was created in MNI space.

Object maps were created by segmenting MRIs into gray matter, white matter, and CSF. This binarised gray matter map was convolved with the latest version of a probabilistic brain atlas(Hammers *et al*, 2003) to create individualized object maps of volumes of interest as previously described (Edison *et al*, 2007).

We then sampled the [^{11}C](R)PK11195 binding maps and RATIO images using Analyze AVW 8.1 in the following regions: whole cortex, frontal, temporal, parietal and occipital association cortices, anterior and posterior cingulate gyrus, striatum, and thalamus. A sub-regional analysis of the temporal lobe was also performed. Levels of microglial activation and amyloid load in the hippocampus, parahippocampal gyrus, amygdala and middle and inferior temporal gyrus were also computed.

Statistical parametric mapping (SPM) analysis. Parametric images were smoothed with $6\,mm \times 6\,mm \times 6\,mm$ kernel filter before SPM analysis. Significant increases in microglial activation, amyloid load, and glucose metabolism in patients compared with control subjects were localized using a voxel threshold of $P < 0.005$ and cluster extent threshold of 50 voxels. If there was no significant cluster at the above-defined threshold, voxel threshold was dropped to $P < 0.05$ and cluster extent threshold of 50 voxels in order to detect small changes. Significant differences in levels of microglial activation and glucose metabolism between PDD and PD were interrogated using a voxel threshold of $P < 0.05$ and extent threshold of 50 voxels. Statistical maps were corrected for multiple comparisons using cluster-level inference derived from random field theory as implemented in SPM.

As ROI analysis evaluates larger cortical regions, to evaluate smaller changes in microglial activation, glucose metabolism, and amyloid load, each single subject was compared against the corresponding control group for all the three tracers using SPM.

Statistical analysis. Statistical interrogations of ROI data were performed using SPSS for Windows version 19 (SPSS, Chicago, Illinois, USA). From past experience and on theoretical grounds, we expected only increases in [^{11}C]PIB uptake and [^{11}C](R)PK11195 BP in PDD compared with controls, then we used one-tailed Student's *t*-tests to interrogate the ROI data. The correlation between microglial activity and cognitive scores was tested pixel-by-pixel using SPM where pixel-wise BP of [^{11}C](R)PK11195 PET was the dependent variable and the mini-mental state examination (MMSE) scores were the covariate of interest. Similarly, correlation between glucose metabolism and cognitive scores were tested using SPM where pixel-wise rCMRGlc was the dependent variable and the MMSE scores were the covariate of interest. Additionally, we have performed correlation between [^{11}C](R)PK11195 BP and rCMRGlc for individual subject for each of multiple regions.

RESULTS

[^{11}C](R)PK11195 PET

Supplementary Table S1 shows the demographic details of the subjects, while Supplementary Table S2 shows the

details of neuropsychometric tests. The mean regional [11C](*R*)PK11195 BPs for the PDD, PD, and control subjects are detailed in Table 1a. The PDD patients showed a statistically significant 35–65% increase of [11C](*R*)PK11195 BP in different cortical and subcortical regions. Individually, six PDD subjects showed significant increases (more than mean control BP + 2SD) in these regions. The PD subjects showed a statistically significant 25–30% increase of microglial activation in the temporal and occipital regions. The frontal and parietal regions also showed increases in microglial activity but just below the statistical threshold for significance (frontal cortex, $P = 0.064$; and parietal cortex, $P = 0.06$). Individually, three of the PD subjects showed significant increases (more than mean control BP + 2SD) in microglial activation in the anterior and posterior cingulate and frontal, temporal, parietal, and occipital cortical regions.

Figure 1a shows the SPM analysis comparing [11C](*R*)PK11195 BP increases in the 11 PDD subjects compared with 10 control subjects. SPM shows significant increases in microglial activity in frontal, temporal, parietal, and occipital cortical regions at a voxel threshold of $P < 0.005$ and extent threshold of 50 voxels. Details of the cortical regions with increased uptake are shown in Table 2a. Figure 1b demonstrates significant increases in [11C](*R*)PK11195 BP for eight PD subjects compared with 10 control subjects in temporal, parietal, and occipital cortical regions at voxel threshold of $P < 0.005$ and an extent threshold of 50 voxels. Table 2b details the significant clusters detected using SPM. The comparison between PDD and PD subjects with a threshold of $P < 0.05$ and extent threshold of 50 voxel revealed a significant relative increase in BP in PDD in the left parietal lobe (MNI coordinates -30, -34, 54) with a cluster size of 5387 voxels ($P < 0.0001$; Figure 2a). SPM analysis of single subjects demonstrated significant increase in microglial activation in 10 PDD subjects, while all PD subjects except one demonstrated significant increase in microglial activation. Figure 4 is an example of increases in microglial activation in a single PDD and a PD subject using 'single-subject SPM analysis'.

[11C]PIB-PET

The details of [11C]PIB uptake ratios in PDD subjects and PD subjects in comparison to the control subjects are given in Table 1b. All subjects had an [11C]PIB uptake RATIO of < 1.4 in cortical regions except for one PD subject where the [11C]PIB uptake was increased in posterior cingulate and one PDD subject who showed an uptake ratio of 1.5 in the occipital cortical region. Interestingly, this PDD patient showed a reduction in glucose metabolism (rCMRGlc = 0.16, where mean -2SD was 0.186) in the anterior temporal lobe. SPM did not detect any significant increase in the [11C]PIB uptake between PD and controls nor PDD and controls as a group. Single-subject SPM analysis demonstrated that eight PDD subjects and two PD subjects showed significant increase in amyloid. When amyloid load was present, it was predominantly in the cortical regions, including anterior and posterior cingulate cortices. However, subjects who did not have any amyloid load did have increased microglial activation and reduced

glucose metabolism in the temporo-parietal cortical regions.

[18F]FDG PET

The regional cortical rCMRGlc for 11 PDD and six PD subjects are given in Table 1c. PDD subjects showed significant reductions in glucose metabolism compared with the control subjects in the posterior cingulate, temporal, parietal, and occipital cortical regions. Interestingly, parieto-occipital hypometabolism was significantly decreased compared with the temporal region. Individually 9 out of the 11 PDD patients showed a significant reduction in glucose metabolism in the parieto-occipital or posterior cingulate. Neuropsychometric scores did not correlate with the cerebral glucose metabolism.

SPM analysis (illustrated in Figure 3a) also showed a significant reduction in glucose metabolism in PDD subjects compared with the control subjects in frontal, temporal, parietal, and occipital regions at a voxel threshold of $P < 0.005$. There were two large clusters with a *Z*-score of 5.97 and cluster size 83 154 one on either side with a corrected $P < 0.0001$. SPM analysis revealed reductions in glucose metabolism in the temporal, parietal, occipital, and also in the frontal cortical regions for the PD cohort using a cluster threshold of $P < 0.05$. (Due to technical reasons, we were unable to estimate two PD subjects' rCMRGlc.) Results from the SPM analysis are illustrated in Figure 3b and significantly reduced clusters are listed in Supplementary Table S3. An SPM comparison between PDD and PD subjects with a threshold of $P < 0.05$ and extent threshold of 50 voxel showed that there was a significant relative reduction of glucose metabolism in frontal, temporal, parietal, and occipital cortical regions in PDD compared with PD subjects (see Figure 2b). SPM revealed large clusters of reduced rCMRGlc (95409 voxels, corrected $P < 0.0001$) covering both hemispheres. Single-subject SPM analysis demonstrated clusters of reduced rCMRglc for all PD and PDD subjects, with PDD subjects showing even greater reduction in glucose metabolism compared with PD subjects. Figure 4 demonstrates reduction in glucose metabolism in single PDD and PD subjects compared with control subjects.

Correlation between MMSE Scores, [11C](*R*)PK11195 BP, and rCMRGlc

Pixel-by-pixel correlation between microglial activation and MMSE scores demonstrated an inverse correlation between cortical microglial activation (temporo-parietal, occipital, and frontal) and MMSE scores. Similarly, temporo-parietal and occipital reduction in rCMRGlc was correlated with MMSE scores. Figure 5a demonstrates the significant clusters of microglial activation using regression analysis of [11C](*R*)PK11195 BP against MMSE score in 11 PDD subjects at a cluster threshold of $P < 0.00005$ with extent threshold of 200 voxels, where cortical microglial activation was inversely correlated with MMSE in PDD subjects. Figure 5b demonstrates the significant clusters using regression analysis of rCMRGlc against MMSE score in 11 PDD subjects at a cluster threshold of $P < 0.00005$ with extent threshold of 200 voxels. The details of the

Table 1 Regional Microglial Activation, Amyloid Load, and Glucose Metabolism in PDD and PD Subjects

	Anterior cingulate gyrus	Posterior cingulate gyrus	Thalamus	Striatum	Frontal cortex	Temporal cortex	Parietal cortex	Occipital cortex	Whole cortex
(a) [¹¹C](R)PK11195 binding potential in PDD and PD subjects compared with controls									
PDD									
Mean	0.50	0.58	0.52	0.50	0.49	0.46	0.47	0.52	0.49
SD	0.20	0.21	0.22	0.18	0.18	0.14	0.16	0.14	0.16
P-value	0.04*	0.02*	0.28	0.001*	0.01*	0.02*	0.01*	0.01*	0.01*
% Increase	35	39	10	65	52	32	48	37	41
PD									
Mean	0.43	0.51	0.51	0.38	0.42	0.44	0.42	0.49	0.44
SD	0.18	0.17	0.17	0.14	0.15	0.10	0.15	0.12	0.13
P-value	0.19	0.11	0.30	0.10	0.06	0.03*	0.06	0.02*	0.05*
% Increase	18	21	9	25	30	25	33	30	28
HC									
Mean	0.37	0.42	0.47	0.30	0.32	0.35	0.32	0.38	0.35
SD	0.10	0.10	0.14	0.08	0.08	0.08	0.10	0.08	0.09

	Anterior cingulate gyrus	Posterior cingulate	Thalamus	Striatum	Frontal cortex	Temporal cortex	Parietal cortex	Occipital cortex
(b) [¹¹C]PIB uptake in PDD, PD subjects, and healthy controls (HC)								
PDD								
Mean	1.15	1.17	0.97	1.15	1.14	1.11	1.11	1.17
SD	0.14	0.09	0.13	0.11	0.12	0.09	0.10	0.14
P-value	0.14	0.03*	0.21	0.10	0.11	0.06	0.15	0.12
% Increase	5	6	-4	4	5	5	3	5
PD								
Mean	1.15	1.19	1.08	1.15	1.16	1.11	1.17	1.19
SD	0.13	0.18	0.10	0.10	0.11	0.09	0.12	0.10
P-value	0.16	0.10	0.04*	0.11	0.04*	0.08	0.03*	0.03*
% Increase	5	8	8	5	7	5	9	8
HC								
Mean	1.10	1.10	1.00	1.10	1.08	1.06	1.07	1.11
SD	0.09	0.08	0.07	0.05	0.06	0.04	0.05	0.05

|	Anterior cingulated gyrus	Posterior cingulated gyrus	Thalamus	Striatum	Frontal cortex	Temporal cortex	Parietal cortex	Occipital cortex	Med temp cortex	Whole cortex
(c) Significant areas of elevated [¹¹C](R)PK11195 BP in PDD subjects compared with controls localized by SPM										
PDD										
Mean	0.27	0.30	0.21	0.30	0.26	0.21	0.24	0.23	0.19	0.24
SD	0.04	0.04	0.04	0.04	0.04	0.03	0.04	0.05	0.03	0.04
P-value	0.081	0.014*	0.001*	0.19	0.07	0.0003*	0.006*	0.0002*	0.002*	0.004*
% Decrease	9	13	37	6	9	23	17	31	17	17
PD										
Mean	0.31	0.34	0.25	0.31	0.26	0.30	0.29	0.29	0.211	0.28
SD	0.43	0.05	0.02	0.05	0.03	0.02	0.04	0.05	0.01	0.03
P-value	0.18	0.35	0.04*	0.32	0.10	0.30	0.27	0.29	0.18	0.34
% Decrease	−6	−3	14	4	−6	2.5	−4	−4	4	−2
HC										
Mean	0.29	0.34	0.29	0.32	0.29	0.26	0.28	0.30	0.22	0.28
SD	0.03	0.03	0.05	0.04	0.02	0.02	0.02	0.02	0.02	0.02

* *P* ≤ 0.05.

coordinates are given in Supplementary Table S4. Cortical rCMRGlc was correlated with the MMSE scores. However, we did not demonstrate significant inverse correlation between microglial activation and rCMRGlc in the cortical region using ROI analysis. In Figure 6, we have overlaid SPM maps of microglial activation and glucose metabolism on SPM templates, which indicates that there is significant overlap between microglial activation and glucose metabolism in several cortical regions; however, there were areas where microglial activation and glucose metabolism were disconnected.

DISCUSSION

In this study, we have demonstrated that cortical microglial activation is increased in both PDD and PD subjects compared with healthy control subjects, the spatial extent of
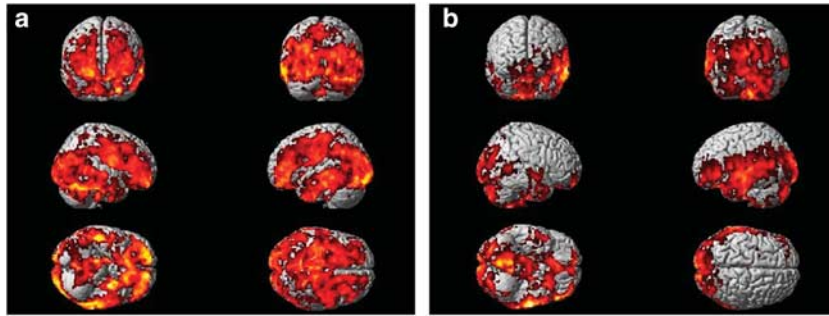
Figure 1 [^{11}C](*R*)PK11195 uptake in PDD and PD subjects compared with controls. (a) [^{11}C](*R*)PK11195 uptake in 11 PDD subjects compared with 10 control subjects showing significant increase in microglial activity in frontal, temporo-parietal, and occipital cortical regions at a $P<0.005$ and extent threshold of 50 voxels. (b) [^{11}C](*R*)PK11195 uptake in eight PD subjects compared with 10 control subjects showing significant increase in microglial activity in temporo-parietal and occipital cortical regions at a $P<0.005$ and extent threshold of 50 voxels.
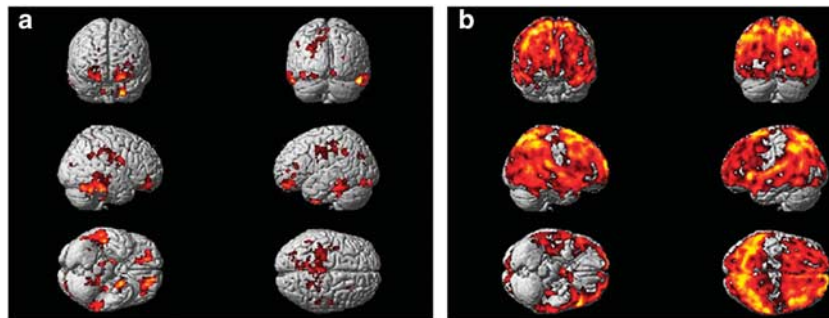
Figure 2 Statistical parametric mapping (SPM) analysis of [^{11}C](*R*)PK11195 BP and rCMRGlc between PDD and PD subjects. (a) SPM analysis of [^{11}C](*R*)PK11195 BP between PDD and PD subjects. Shows minimally increased microglial activity in PDD compared with PD using [^{11}C](*R*)PK11195 in11 PDD subjects compared with 8 PD subjects at voxel threshold of $P<0.05$ and extent threshold of 50 voxels. (b) SPM analysis of rCMRGlc between PDD and PD subjects. Shows significantly reduced glucose metabolism in PDD compared with PD using [^{18}F]FDG PET in11 PDD subjects compared with 6 PD subjects at voxel threshold of $P<0.05$ and extent threshold of 50 voxels.
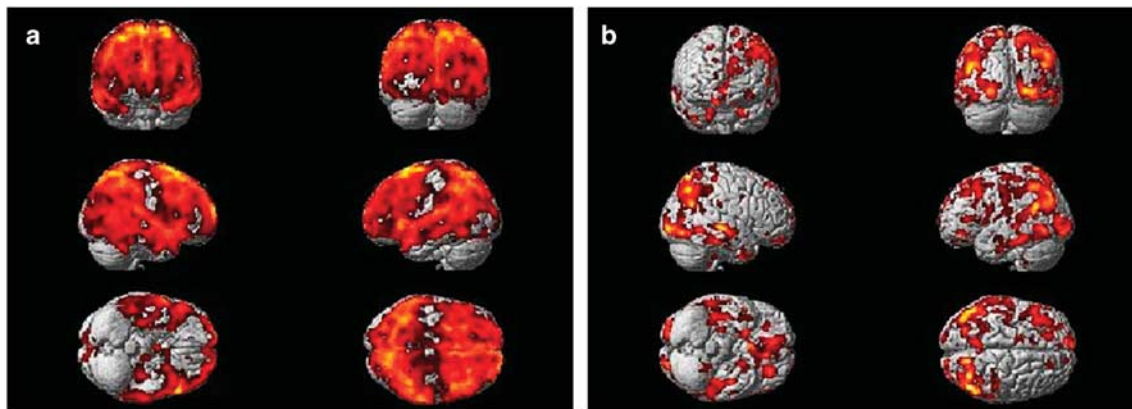
Figure 3 Statistical parametric mapping (SPM) analysis of rCMRGlc in PDD and PD subjects compared with the controls. (a) Reduction in rCMRGlc in 11 PDD subjects compared with eight control subjects showing significant reduction in frontal, temporo-parietal, and occipital region at voxel threshold of $P<0.005$ and extent threshold of 50 voxels. (b) Reduction in rCMRGlc in eight PD subjects compared with eight control subjects showing significant reduction in frontal, temporo-parietal, and occipital region at voxel threshold of $P<0.05$ and extent threshold of 50 voxels.

the activation being greater in PDD where brainstem was also involved. Maximal microglial activation was detected in parieto-occipital cortex but frontal, temporal and anterior and posterior cingulate cortical regions also showed significant increases. Using [^{11}C]PIB as a PET marker for fibrillar β amyloid, we were able to detect increases in

amyloid as a group both in PDD and PD. Using group mean ROI analysis, rCMRGlc was reduced in posterior cingulate, temporal, parietal, and occipital cortical regions in the PDD subjects compared with controls. The majority of the PDD subjects individually showed a reduction in glucose metabolism in the hippocampus and in the temporo-parietal

**Table 2** Areas of Elevated Microglial Activation in PDD and PD

Region	Coordinates			Z-score	Corrected P-value	Cluster size
	x	y	z			
(a) Significant areas of elevated [¹¹C](R)PK11195 BP in PDD subjects compared with controls as localized by SPM (P<0.005 extent threshold 50 voxels). (Corrected threshold of P<0.005 at cluster level and extent threshold of 50 voxels).						
Left posterior temporal gyrus	−68	−38	−10	4.23	<0.0001	777
Left precentral gyrus	−30	−28	56	4.18	<0.0001	6020
Right lateral gyrus (occipital lobe)	40	−90	−14	4.10	<0.0001	725
Left lateral occipito temporal gyrus	−30	−6	−44	3.99	<0.0001	2402
Left parahippocampal gyrus	−30	−2	−30	3.97	<0.0001	2402
Left lateral gyrus (occipital lobe)	−26	−98	−10	3.94	<0.0001	711
Brainstem	12	−26	−14	3.71	<0.0001	1315
Left middle and inferior temporal gyrus	−60	−34	−26	3.61	<0.0001	777
Right orbitofrontal gyrus	22	54	−14	3.56	<0.0001	749
Right precentral gyrus	50	2	24	3.47	0.001	640
Right middle frontal gyrus	20	42	−2	3.37	<0.0001	749
(b) Significant areas of elevated [¹¹C](R)PK11195 BP in PD subjects compared with controls as localized by SPM (P<0.005 extent threshold 50 voxels).						
Left middle and inferior temporal gyrus	−64	−18	−10	4.64	<0.0001	1483
Left inferior frontal gyrus	−52	32	−8	4.36	0.024	318
Left superior temporal gyrus	−66	−26	−2	4.19	<0.0001	1483
Left orbitofrontal gyrus	−34	58	−14	3.50	<0.0001	318
Left cuneate gyrus	0	−92	20	3.46	0.024	789

and occipital regions. We have also demonstrated temporo-parietal hypometabolism in the non-demented PD patients using SPM analysis.

This study demonstrated significant cortical microglial activation in both non-demented and demented PD subjects. This may suggest that neuroinflammation could be an early phenomenon in this disease spectrum and may appear even before the onset of dementia and could persist as the disease advances. Neuroinflammation is the defense mechanism of living brain for external injury and acts in two ways: either by rescuing damaged cells or by further destroying them depending on the anti-inflammatory and pro-inflammatory properties of the cytokines released. When microglia are activated, expressing the TSPO, they become phagocytic and release a variety of cytokines such as TNFα, IL1, IL2, IL6, and NO. It is suggested that these substances can be involved in cellular injury and neuronal degeneration or can act as growth factors. It is shown that in degenerative disease like AD, activated microglia and raised cytokine levels are present around the senile plaques, stimulating amyloid precursor protein production, which, in turn, leads to excessive production of β-amyloid. The β-amyloid fibrils, in turn, cause further microglial activation, resulting in a vicious cycle.

Like senile plaques, the aggregated α-synuclein in Lewy bodies attracts activated microglia potentially leading to neuronal death and driving disease progression (Zhang et al, 2005). As a group, there was increased microglial activity in cortical association regions in both PD and PDD subjects, more extensive in the latter, but individual analyses showed some variability between subjects. There was some discrepancy between the number of subjects who

demonstrated increased microglial activation between ROI analysis and single-subject SPM analysis. This could partly be due to the relatively large regions included in the ROI analysis, while SPM analysis picks up the clusters that demonstrates significant microglial activation. One possible explanation for variability in microglial activation could be due to the heterogeneity of the subjects and variability in cortical levels of Lewy body pathology present in different subjects. It may be possible that microglia may become activated with some toxic insult, and when the toxic insult is over, microglia could return to dormant stage. Once microglia are activated, release of cytokines and toxic substances may cause neuronal damage but one could speculate that even if the microglial activation then subsides the neuronal damage continues as apoptotic cascades are already initiated. A previous study from our unit reported that PD patients without dementia did not show a significant difference in cortical microglial activation over a period of time, in support of this point of view. Here, we have now shown that cortical microglial activity is significantly increased both in non-demented and demented PD subjects. This may suggest that early and persistent microglial activation may be one of the factors influencing progressive cognitive dysfunction in this disease spectrum. However, one could also argue that microglial activation in PD may not be associated with dementia. McGeer et al (2003) has demonstrated the presence of microglilal activation and dopaminergic cell loss in the Substantia Nigra of monkeys after 5.5–14 years following brief exposure to MPTP (1-methyl-4-phenyl-1,2,3,6-tetrahydro-pyridine), suggesting even if the initial insult is over, microglial activation and neuronal damage could continue.
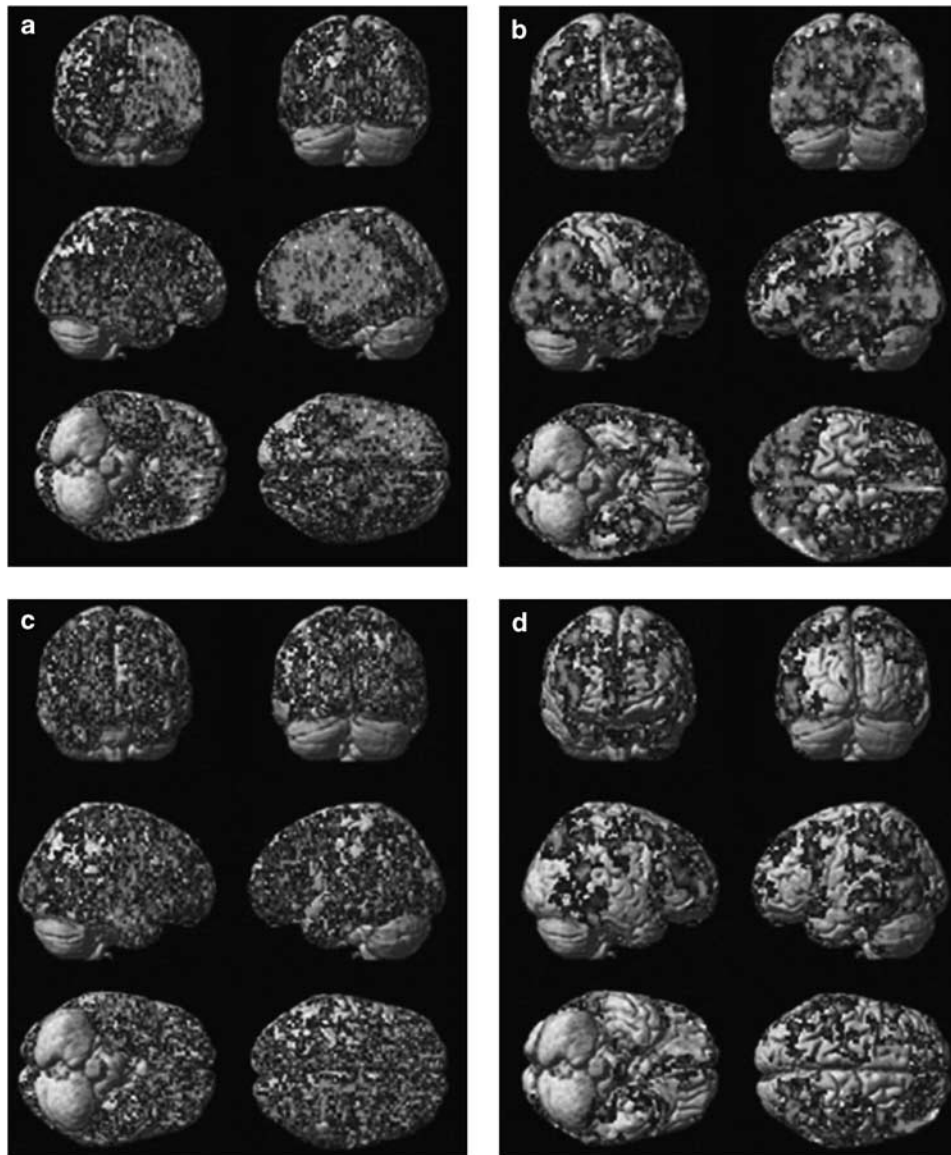
Figure 4   Single subject SPM analysis of microglial activation and glucose metabolism in PDD and PD subjects against controls. (a, b) Increased microglial activation and reduced glucose metabolism, respectively, in a PDD. (c and d) Increased microglial activation and reduction in glucose metabolism in PD subject.

It is also suggested that microglial activation could be episodic causing progressive neuronal loss, and eventually reactive microglia could burn out, while the neuronal damage continues. However, microglial activation in PD cannot be explained by this as these subjects have significantly less cortical atrophy compared with the PDD subjects (data not presented in this paper). Our failure to detect activated microglia in all subjects with PDD could reflect either insufficient sensitivity of the [^{11}C](R)PK11195 PET approach and/or the presence of other processes responsible for neuronal damage. The latter could involve activation of astrocytes by the cortical Lewy body pathology or initiation of autophagy and apoptotic cascades. Alternatively, microglial activation could switch on and off depending on the nature of the insult—it is known that after stroke microglial activation eventually subsides. Recent study in a small number of subjects have demonstrated that

microglial activation is also elevated in subjects with Lewy body dementia (Iannaccone *et al*, 2012)

A previous study from our group of non-demented PD subjects reported the presence of raised microglial activity in subcortical regions, including striatum, pallidum, thalamus, and pons along with cortical regions (Gerhard *et al*, 2006). We have replicated those findings in this new study with ROI analysis. Minor variations in the statistical significance could be due to the heterogeneity of the subjects in these two studies.

In this study, our PDD patients showed a reduction in cortical glucose metabolism, particularly in temporo-parietal and occipital regions. Widespread cortical hypometabolism with particularly severe involvement of the temporo-parietal areas have been reported in earlier studies in PDD (Klein *et al*, 2010; Peppard *et al*, 1990; Vander Borght *et al*, 1997). Studies have also noted cortical
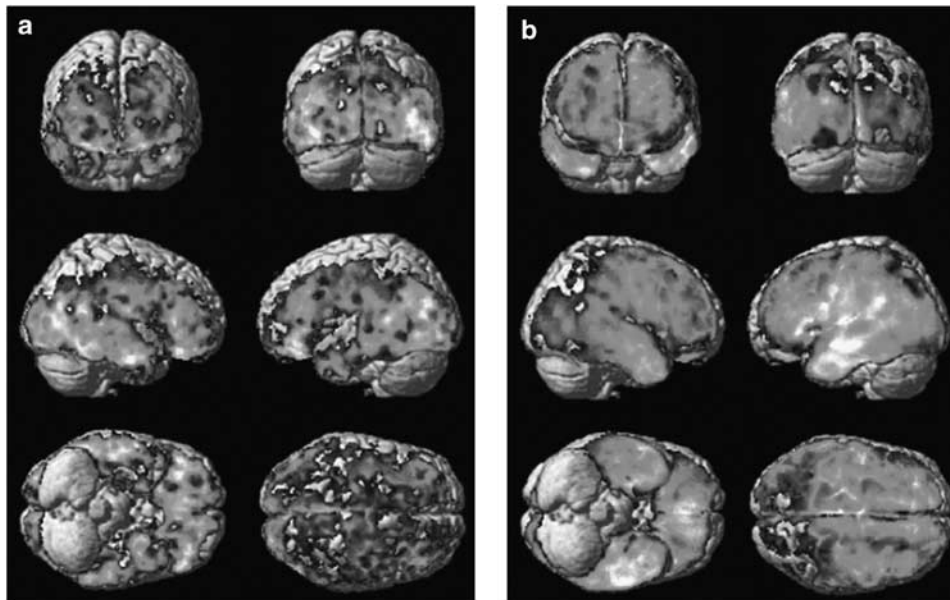
Figure 5 Pixel-by-pixel correlation between microglial activation, glucose metabolism, and MMSE scores in PDD subjects. (a) Significant clusters using regression analysis of [^{11}C](*R*)PK11195 BP against MMSE score in 11 PDD subjects at a cluster threshold of $P < 0.00005$ with extent threshold of 200 voxels. Cortical microglial activation was correlated with MMSE in PDD subjects. (b) Significant clusters using regression analysis of rCMRGlc against MMSE score in 11 PDD subjects at a cluster threshold of $P < 0.00005$ with extent threshold of 200 voxels. Cortical rCMRGlc was correlated with the MMSE scores.
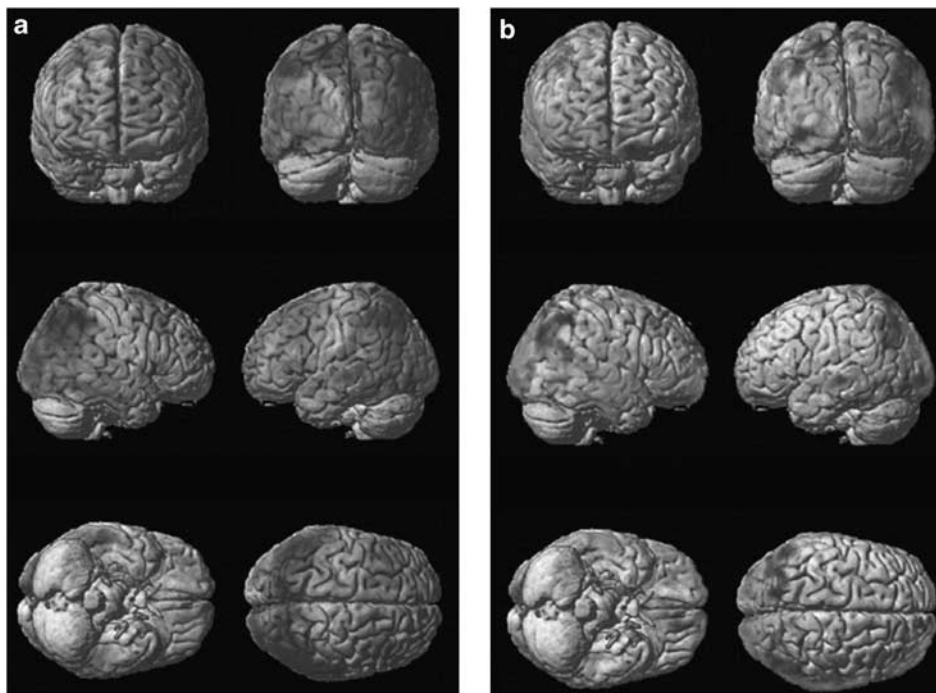
Figure 6 Semi-quantitative figure showing microglial activation *vs* hypometabolism overlaid on SPM templates. (a) [^{11}C](*R*)PK11195 BP map overlaid on rCMRGlc map in PDD, (b) the same in a PD subject. Microglial activation is represented in red, rCMRglc in blue, while purple demonstrates the overlap.

involvement, particularly temporo-parietal areas in non-demented PD patients, but to a lesser degree compared with PDD (Hu *et al*, 2000). We have also demonstrated that reductions in glucose metabolism can be detected in non-demented PD subjects using SPM analysis. Even though the number of subjects studied in this project are small, this may suggest that cortical neuronal dysfunction as evidenced by reduced glucose metabolism is present in PD, even

without significant cognitive impairment. The lack of significant difference in ROI analysis could be due to the involvement of relatively smaller areas (clusters) rather than involvement of larger predefined regions. Although PD traditionally has been defined by its characteristic motor hallmarks, non-motor features such as cognitive impairment and dementia are increasingly recognized as part of PD. Mild cognitive impairment is common in non-demented PD

patients, occurring in about 20–50%. It is possible that some of the PD subjects in this study could be in the transitional phase between PD and PDD.

Reduction in cortical hypometabolism has been previously reported in PD subjects (Borghammer et al, 2010). Some studies have also reported hypermetabolism in subcortical structures. Borghammer et al (2009) have demonstrated that these hypermetabolism found in PD could be due to the global mean normalization used in the analysis. They have also demonstrated that depending on the type of analysis used, even the extent of the hypometabolism could vary. Here we have quantitatively evaluated cerebral glucose metabolism using spectral analysis, and the data was not normalized to global mean.

In this study, reductions in cortical glucose metabolism were associated with increases in microglial activation across the combined PD and PDD cohorts. Except for the presence of a small focal increase in anterior cingulate [11C]PIB uptake in one subject, raised amyloid load did not appear to be associated with PDD using ROI analysis. Individual SPM analysis at a threshold of $P < 0.05$ demonstrated that eight PDD subjects and four PD subjects have minimal amount of amyloid, even though these increases were not obvious in the ROI analysis. In a previous study, we have found 20% of PDD subjects had increased cortical amyloid using ROI analysis. Recently published [11C] PIB studies (Gomperts et al, 2008; Maetzler et al, 2009; Maetzler et al, 2008) have also reported increased amyloid load in PDD subjects. It is also reported that in [11C]PIB + ve subjects in PDD and DLB, ApoE4 prevalence was higher, CSF Abeta42 levels were lower, and, among demented subjects, [11C]PIB binding was associated with a lower MMSE score, suggesting LBD subjects with cortical β-amyloid show characteristics usually observed in AD (Maetzler et al, 2009). Motor symptoms were not associated with [11C]PIB binding in this study. Neuropathological studies have reported that striatal amyloid can be found in PDD; however, this is usually diffuse rather than fibrillar in nature and does not necessarily bind thioflavin ligands such as [11C]PIB (Jellinger and Attems, 2006; Liang et al, 2006). This may explain the lower prevalence of amyloid in PDD reported in PET studies compared with pathological series.

Our findings suggest that persistent microglial activation along with small amount of fibrillar amyloid load is associated with the neuronal damage and reduction in glucose metabolism in PDD. Studies in Lewy body dementia using [11C]PIB PET has demonstrated abundant amyloid. Even though not supported by the presented data, it is feasible that the presence of amyloid could accelerate the dementing process in DLB. In this disease spectrum, apart from amyloid pathology, loss of cholinergic and monoaminergic projections could also contribute to cognitive difficulties.

In this study, for the first time, we have also demonstrated a correlation between cortical microglial activation and MMSE, further suggesting that microglial activation may be associated with neuronal damage in PDD. However, we did not find such a correlation with other memory test scores. We were also able to demonstrate that there was a correlation between cerebral hypometabolism and MMSE, which is well established.

LIMITATIONS

One of the limitation of this study is the small number of subjects studied in each group. This study is a triple tracer study, and due to the intensity of the scanning involved, we were not able to include large number of subjects. However, in this preliminary study, we were able to demonstrate novel findings, which forms the basis of larger studies. Although [11C](R)PK11195 PET is a measure of microglial activation, it has relatively low in vivo specific binding. One study evaluating [11C](R)PK11195 PET and [11C]PBR28 PET has demonstrated that in vivo binding of [11C](R)PK11195 PET is 80-fold lower than second generation TSPO tracer, [11C]PBR28. It is also suggested that this relatively low in vivo specific binding of [11C](R)PK11195 PET may have obscured the detection of non-binding in peripheral organs. To gain insight into this issue, we are now evaluating different types of dementia with the novel TSPO tracers.

In conclusion, we have demonstrated that cortical microglial activation and reduced glucose metabolism can be detected in PD and PDD subjects. Microglial activation was inversely correlated with MMSE, while rCMRGlc was correlated with MMSE. Given this, agents that suppress or reverse microglial activation could be a potential protective treatment for neurodegenerative diseases like PDD but, if they were to be effective, would need to be started ahead of the appearance of dementia.

DISCLOSURE

Dr Edison has received funding from Medical Research Council, UK for his fellowship. Professor Brooks was also the chief medical officer for GE healthcare, and he has received consultancy fees/honoraria from the following: Acadia Pharmaceuticals Inc, Amsterdam Molecular Therapeutics (AMT) BV, AstraZeneca, BiogeIdec,NeuroNova AB, Eli Lilly and Company, Medtronic Inc, Shire Pharmaceuticals Inc, Synosia Therapeutics AG, GlaxoSmith Kline, UBC Biosciences Inc, Veralis (R&D) limited, Genentech Inc, Navidea. Dr K Ray Chaudhuri has received honoraria for lectures at sponsored symposia from UCB, Britannia, GSK, Abbott pharmaceuticals, and has been supported by educational grants from Abbott, UCB, Boehringer-Ingelheim. Dr Walker has received consultancy and speaker fees and research support from GE Healthcare, consultancy fees from Bayer Healthcare, and research support from Lundbeck. Dr Ahmed was funded by Parkinson's research, UK, Dr Gelosa, Dr Fan, and Dr Turkheimer have nothing to disclose.

REFERENCES

Anderson AN, Pavese N, Edison P, Tai YF, Hammers A, Gerhard A et al (2007). A systematic comparison of kinetic modelling

methods generating parametric maps for [(11)C]-(R)-PK11195. *Neuroimage* **36**: 28–37.

Banati RB, Newcombe J, Gunn RN, Cagnin A, Turkheimer F, Heppner F *et al* (2000). The peripheral benzodiazepine binding site in the brain in multiple sclerosis: quantitative *in vivo* imaging of microglia as a measure of disease activity. *Brain* **123** (Pt 11) 2321–2337.

Berding G, Odin P, Brooks DJ, Nikkhah G, Matthies C, Peschel T *et al* (2001). Resting regional cerebral glucose metabolism in advanced Parkinson's disease studied in the off and on conditions with [(18)F]FDG-PET. *Mov Disord* **16**: 1014–1022.

Borghammer P, Chakravarty M, Jonsdottir KY, Sato N, Matsuda H, Ito K *et al* (2010). Cortical hypometabolism and hypoperfusion in Parkinson's disease is extensive: probably even at early disease stages. *Brain Struct Funct* **214**: 303–317.

Borghammer P, Cumming P, Aanerud J, Forster S, Gjedde A (2009). Subcortical elevation of metabolism in Parkinson's disease–a critical reappraisal in the context of global mean normalization. *Neuroimage* **47**: 1514–1521.

Brix G, Zaers J, Adam LE, Bellemann ME, Ostertag H, Trojan H *et al* (1997). Performance evaluation of a whole-body PET scanner using the NEMA protocol. National Electrical Manufacturers Association. *J Nucl Med* **38**: 1614–1623.

Cummings JL (1988). Intellectual impairment in Parkinson's disease: clinical, pathologic, and biochemical correlates. *J Geriatr Psychiatry Neurol* **1**: 24–36.

Cunningham VJ, Jones T (1993). Spectral analysis of dynamic PET studies. *J Cereb Blood Flow Metab* **13**: 15–23.

Eberling JL, Richardson BC, Reed BR, Wolfe N, Jagust WJ (1994). Cortical glucose metabolism in Parkinson's disease without dementia. *Neurobiol Aging* **15**: 329–335.

Edison P, Archer HA, Gerhard A, Hinz R, Pavese N, Turkheimer FE *et al* (2008a). Microglia, amyloid, and cognition in Alzheimer's disease: An [11C](R)PK11195-PET and [11C]PIB-PET study. *Neurobiol Dis* **32**: 412–419.

Edison P, Archer HA, Hinz R, Hammers A, Pavese N, Tai YF *et al* (2007). Amyloid, hypometabolism, and cognition in Alzheimer disease: an [11C]PIB and [18F]FDG PET study. *Neurology* **68**: 501–508.

Edison P, Rowe CC, Rinne JO, Ng S, Ahmed I, Kemppainen N *et al* (2008b). Amyloid load in Parkinson's disease dementia and Lewy body dementia measured with [11C]PIB positron emission tomography. *J Neurol Neurosurg Psychiatry* **79**: 1331–1338.

Emre M, Aarsland D, Brown R, Burn DJ, Duyckaerts C, Mizuno Y *et al* (2007). Clinical diagnostic criteria for dementia associated with Parkinson's disease. *Mov Disord* **22**: 1689–1707.

Feng T, Wang Y, Ouyang Q, Duan Z, Li W, Lu L *et al* (2008). Comparison of cerebral glucose metabolism between multiple system atrophy Parkinsonian type and Parkinson's disease. *Neurol Res* **30**: 377–382.

Gerhard A, Pavese N, Hotton G, Turkheimer F, Es M, Hammers A *et al* (2006). *In vivo* imaging of microglial activation with [11C](R)-PK11195 PET in idiopathic Parkinson's disease. *Neurobiol Dis* **21**: 404–412.

Gomperts SN, Rentz DM, Moran E, Becker JA, Locascio JJ, Klunk WE *et al* (2008). Imaging amyloid deposition in Lewy body diseases. *Neurology* **71**: 903–910.

Hammers A, Allom R, Koepp MJ, Free SL, Myers R, Lemieux L *et al* (2003). Three-dimensional maximum probability atlas of the human brain, with particular reference to the temporal lobe. *Hum Brain Mapp* **19**: 224–247.

Hirsch EC, Breidert T, Rousselet E, Hunot S, Hartmann A, Michel PP (2003). The role of glial reaction and inflammation in Parkinson's disease. *Ann NY Acad Sci* **991**: 214–228.

Hosokai Y, Nishio Y, Hirayama K, Takeda A, Ishioka T, Sawada Y *et al* (2009). Distinct patterns of regional cerebral glucose

metabolism in Parkinson's disease with and without mild cognitive impairment. *Mov Disord* **24**: 854–862.

Hu MT, Taylor-Robinson SD, Chaudhuri KR, Bell JD, Labbe C, Cunningham VJ *et al* (2000). Cortical dysfunction in non-demented Parkinson's disease patients: a combined (31)P-MRS and (18)FDG-PET study. *Brain* **123**, Pt 2 340–352.

Hughes TA, Ross HF, Musa S, Bhattacherjee S, Nathan RN, Mindham RH *et al* (2000). A 10-year study of the incidence of and factors predicting dementia in Parkinson's disease. *Neurology* **54**: 1596–1602.

Iannaccone S, Cerami C, Alessio M, Garibotto V, Panzacchi A, Olivieri S *et al* (2012). *In vivo* microglia activation in very early dementia with Lewy bodies, comparison with Parkinson's disease. *Parkinsonism Relat Disord* (in press) doi:10.1016/j.parkreldis.2012.07.002.

Jellinger KA, Attems J (2006). Does striatal pathology distinguish Parkinson disease with dementia and dementia with Lewy bodies? *Acta Neuropathol* **112**: 253–260.

Klein JC, Eggers C, Kalbe E, Weisenbach S, Hohmann C, Vollmar S *et al* (2010). Neurotransmitter changes in dementia with Lewy bodies and Parkinson disease dementia *in vivo*. *Neurology* **74**: 885–892.

Klunk WE (2011). Amyloid imaging as a biomarker for cerebral beta-amyloidosis and risk prediction for Alzheimer dementia. *Neurobiol Aging* **32**(Suppl 1): S20–S36.

Klunk WE, Wang Y, Huang GF, Debnath ML, Holt DP, Shao L *et al* (2003). The binding of 2-(4′-methylaminophenyl)benzothiazole to postmortem brain homogenates is dominated by the amyloid component. *J Neurosci* **23**: 2086–2092.

Liang T-W, Noorigian JV, Duda. JE (2006). Does striatal pathology distinguish PDD from DLB? *Mov Disord* **21**(Suppl 13): S69.

Lopresti BJ, Klunk WE, Mathis CA, Hoge JA, Ziolko SK, Lu X *et al* (2005). Simplified Quantification of Pittsburgh Compound B Amyloid Imaging PET Studies: a comparative analysis. *J Nucl Med* **46**: 1959–1972.

Maetzler W, Liepelt I, Reimold M, Reischl G, Solbach C, Becker C *et al* (2009). Cortical PIB binding in Lewy body disease is associated with Alzheimer-like characteristics. *Neurobiol Dis* **34**: 107–112.

Maetzler W, Reimold M, Liepelt I, Solbach C, Leyhe T, Schweitzer K *et al* (2008). [11C]PIB binding in Parkinson's disease dementia. *Neuroimage* **39**: 1027–1033.

McGeer PL, McGeer EG (2004). Inflammation and the degenerative diseases of aging. *Ann N Y Acad Sci* **1035**: 104–116.

McGeer PL, Schwab C, Parent A, Doudet D (2003). Presence of reactive microglia in monkey substantia nigra years after 1-methyl-4-phenyl-1,2,3,6-tetrahydropyridine administration. *Ann Neurol* **54**: 599–604.

Nordberg A, Rinne JO, Kadir A, Langstrom B (2010). The use of PET in Alzheimer disease. *Nat Rev Neurol* **6**: 78–87.

Peppard RF, Martin WR, Carr GD, Grochowski E, Schulzer M, Guttman M *et al* (1992). Cerebral glucose metabolism in Parkinson's disease with and without dementia. *Arch Neurol* **49**: 1262–1268.

Peppard RF, Martin WR, Clark CM, Carr GD, McGeer PL, Calne DB (1990). Cortical glucose metabolism in Parkinson's and Alzheimer's disease. *J Neurosci Res* **27**: 561–568.

Pike KE, Savage G, Villemagne VL, Ng S, Moss SA, Maruff P *et al* (2007). {Beta}-amyloid imaging and memory in non-demented individuals: evidence for preclinical Alzheimer's disease. *Brain* **130**, Pt 11 2837–2844.

Rowe CC, Ellis KA, Rimajova M, Bourgeat P, Pike KE, Jones G *et al* (2010). Amyloid imaging results from the Australian Imaging, Biomarkers and Lifestyle (AIBL) study of aging. *Neurobiol Aging* **31**: 1275–1283.

Sasaki M, Ichiya Y, Hosokawa S, Otsuka M, Kuwabara Y, Fukumura T *et al* (1992). Regional cerebral glucose metabolism in patients with Parkinson's disease with or without dementia. *Ann Nucl Med* **6**: 241–246.

Shah F, Hume SP, Pike VW, Ashworth S, McDermott J (1994). Synthesis of the enantiomers of [N-methyl-^{11}C]PK 11195 and comparison of their behaviours as radioligands for PK binding sites in rats. *Nucl Med Biol* **21**: 573–581.

Spinks TJ, Jones T, Bloomfield PM, Bailey DL, Miller M, Hogg D *et al* (2000). Physical characteristics of the ECAT EXACT3D positron tomograph. *Phys Med Biol* **45**: 2601–2618.

Turkheimer FE, Edison P, Pavese N, Roncaroli F, Anderson AN, Hammers A *et al* (2007). Reference and target region modeling of [^{11}C]-(R)-PK11195 brain studies. *J Nucl Med* **48**: 158–167.

Vander Borght T, Minoshima S, Giordani B, Foster NL, Frey KA, Berent S *et al* (1997). Cerebral metabolic differences in Parkinson's and Alzheimer's diseases matched for dementia severity. *J Nucl Med* **38**: 797–802.

Weiner MW, Veitch DP, Aisen PS, Beckett LA, Cairns NJ, Green RC *et al* (2012). The Alzheimer's Disease Neuroimaging Initiative: a review of papers published since its inception. *Alzheimers Dement* **8**(1 Suppl): S1–S68.

Wyss-Coray T, Mucke L (2002). Inflammation in neurodegenerative disease—a double-edged sword. *Neuron* **35**: 419–432.

Yong SW, Yoon JK, An YS, Lee PH (2007). A comparison of cerebral glucose metabolism in Parkinson's disease, Parkinson's disease dementia and dementia with Lewy bodies. *Eur J Neurol* **14**: 1357–1362.

Zhang W, Wang T, Pei Z, Miller DS, Wu X, Block ML *et al* (2005). Aggregated alpha-synuclein activates microglia: a process leading to disease progression in Parkinson's disease. *Faseb J* **19**: 533–542.